IEEE Access
Multidisciplinary | Rapid Review | Open Access Journal

Received July 9, 2021, accepted July 19, 2021, date of publication July 26, 2021, date of current version July 30, 2021.

Digital Object Identifier 10.1109/ACCESS.2021.3099879

Broadband THz Corrugated Bull's Eye Antennas

DESPOINA KAMPOURIDOU, (Member, IEEE), AND ALEXANDROS FERESIDIS, (Senior Member, IEEE)

Department of Electronic, Electrical and Systems Engineering, University of Birmingham, Edgbaston, Birmingham B15 2TT, U.K.

Corresponding author: Despoina Kampouridou (d.kampouridou@bham.ac.uk)

This work was supported in part by the U.K. Engineering and Physical Sciences Research Council under Grant EP/P008380/1, and in part by the University of Birmingham under a School Postgraduate Scholarship.

ABSTRACT A 3-dB gain and input impedance bandwidth enhancement technique for THz periodically corrugated metallic antennas, also known as Bull's Eye antennas, is presented. A novel design that exploits the depth qualities of the corrugations is introduced, by employing two different depth values for two sets of indented rings. While the gain bandwidth of most single-depth planar corrugated antennas is limited, the 3-dB gain bandwidth of the proposed dual-depth design is expanded along with a high maximum gain. The simulated optimum model of 10 rings at around 300 GHz exhibits a 3-dB gain bandwidth of 8.85% with a maximum gain at broadside of 21.3 dBi. A leaky-wave analysis has been performed via a simple transcendental equation at the level of the gap openings in order to explain the antenna principle of operation. A prototype of the optimum antenna design has been fabricated and measured. The typical subwavelength slot feeding of Bull's eye corrugated antennas is substituted with an easy-to-fabricate open waveguide aperture, yielding a broadband matching performance. Measured results demonstrate a good agreement with simulations and validate the proposed antenna design.

INDEX TERMS Corrugated antennas, Bull's eye, broadband antennas, dual-depth antennas, leaky-wave antennas.

I. INTRODUCTION

The terahertz spectrum is a highly developing frequency band, suitable for a variety of applications including imaging, ultra-high-speed wireless telecommunications and sensing, envisaged to achieve data rates of 100 Gbps or higher. For such emerging technologies, modern antennas usually require high gain, compact size and a broadband gain/directivity performance in order to meet the demands of these THz systems. In addition to the necessity of a broadband gain performance of the antenna, a satisfactory input matching response is desired (typically below -10 dB over a large S_{11} bandwidth), especially in applications where dielectric or other packaging materials are superimposed on the antenna and can potentially affect their radiation. Another significant challenge at the low-THz band is the fabrication complexity and costs that emerge due to the small dimensions of devices and the current limitations of the available fabrication techniques and tools.

Corrugated metallic structures operating at millimeter wave and sub-millimeter wave frequencies have attracted a lot of interest due to their advantages of high gain, low profile, scalable design to lower and higher frequencies and ease of fabrication. It was first observed that a subwavelength aperture on a perfectly conducting metal film boosts dramatically the transmission of light in optical frequencies. This phenomenon is further enhanced when the aperture is surrounded by a set of periodic rings etched off the film [1]–[3]. It has been shown that a narrow directive beam is produced by the excitation of a leaky mode propagating across the corrugations, superimposed on the subwavelength aperture direct radiation [4].

Several high gain antennas and devices based on the enhanced transmission of light principle have been reported in literature including implementations at low THz frequencies [5]–[7]. Other corrugated patterns have found applications in corrugated substrate integrated waveguides (SIWs) for reduced size and broadband SIWs [8] and high-gain leaky wave antennas [9], as well as mechanically rotatable corrugated leaky wave antennas [10] that would enable miniaturization at mm-wave and THz frequencies.

Most of the corrugated antenna implementations, referred to as Bull's Eye antennas, have mainly exploited the periodicity d of the texture for the determination of the operating

The associate editor coordinating the review of this manuscript and approving it for publication was Debdeep Sarkar.

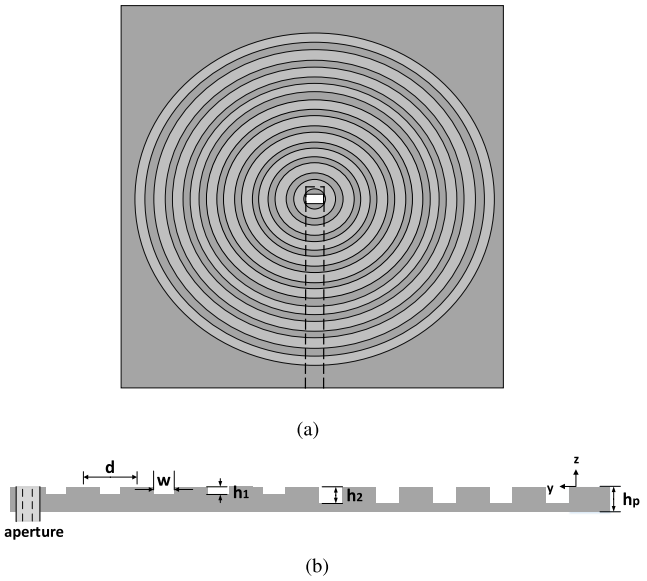

FIGURE 1. Dual-depth Bull's Eye antenna with $r = 10$ rings (a) Front view. (b) Profile corresponding to the dashed lines in (a). Parameters are as $d = 0.961$ mm, $w = 0.611$ mm, $h_p = 0.911$ mm, $h_1 = 0.14$ mm, $h_2 = 0.266$ mm. The dashed line corresponds to a slot aperture and the solid line to an open-ended waveguide aperture.

frequency band, where it should be $d \approx \lambda_0$ for an optimum transmission [5], [11]. However, it has been shown that for a determined value of d, the depth h of the corrugations affects the resonant frequency. This effect has been exploited for only a few applications so far [12]. Furthermore, these antennas are typically excited by a waveguide-fed resonant slot aperture, which offers high gain performance but limits the matching bandwidth as a trade-off. Additionally, the 3-dB gain bandwidth of such antennas is relatively narrow [5], [13]. Some procedures are available in literature for improving the performance, by either modulating the shape of corrugations [14], the width of the gaps [15], or even superimposing corrugated layers [16]–[18]. Although the aperture efficiency has been enhanced in [15] and a dual-band operation has been achieved in [16], there are no techniques for significant improvement of the 3-dB gain bandwidth performance of high gain corrugated antennas, to the best of our knowledge.

In this paper, a novel Bull's Eye antenna is presented at around 300 GHz that achieves a clear gain bandwidth enhancement along with high gain performance. The proposed design, presented in Section II, is a circularly corrugated Bull's Eye type structure of r rings, which employs two different corrugation depth values h_1 and h_2, while the periodicity d is fixed to approximately λ_0 (Fig. 1). The first $r/2$ rings around the feeding aperture use a smaller h value which corresponds to a higher resonant frequency, while the outer $r/2$ rings use a larger h value which corresponds to a lower resonant frequency. In addition, the standard subwavelength slot feeding aperture is replaced with an open-ended waveguide aperture, which is easier to fabricate at low THz and achieves good matching performance [19].

A leaky-wave analysis of the proposed novel dual-depth design is also presented in this paper in Section III, via an analytical periodic method at the level of the gap openings. The dispersion analysis of each single depth antenna predicts the far field behaviour of the dual-depth design, based on the known physics of leaky waves [4], [20].

An optimized model of the proposed antenna with an open-ended waveguide aperture as a feeding technique has been fabricated using CNC metal milling and a split block technique (Section IV). The optimum model with ten rings at 300 GHz exhibits a 3-dB gain bandwidth of 8.85% with 21.3 dBi maximum gain, which is the best reported gain bandwidth performance so far for this type of corrugated antennas of the same size at the low-THz spectrum. Measurements of the fabricated prototype show a very good agreement with simulations of a slightly redesigned model due to fabrication tolerances and validate the performance of the proposed design. The conclusions from this work are drawn in Section V.

II. THE DUAL-DEPTH CONCEPT

The proposed gain bandwidth enhancement technique exploits the relationship between the depth of the corrugations h and the resonant wavelength λ_0 as described in [11]:

$$h \approx \frac{(2n+1)\lambda_0}{4} \tag{1}$$

where n is a non-negative integer. The proposed design consists of a number of rings r, with periodicity d (Fig. 1.b). While keeping d fixed around λ_0, the corrugations' depth h is considered as the only varying parameter for the present study. The first set of $r/2$ unit cells is designed to operate at a frequency f_1 determined only by the depth h_1 and the next set of $r/2$ unit cells with depth h_2 is designed to operate at a frequency f_2.

The corrugated antenna for this study is designed at around 300 GHz, according to the principles set in [21]–[22]. The antenna in all the studies of this Section is fed by a subwavelength slot with dimensions optimized to $(s_x, s_y) = (0.5838 \text{ mm}, 0.159 \text{ mm})$, which is, in turn, fed by a typical WR-3 waveguide on the rear side of the metallic body of the antenna. This optimized slot secures an S_{11} below -10 dB at the operational gain bandwidth, which results in a very similar gain and directivity performance [19].

The whole metallic antenna body has a thickness $h_p = 0.911$ mm, gap-groove distance $w = 0.611$ mm, periodicity $d = 0.961$ mm and overall size of 25×25 mm^2. These dimensions were optimized via an in-house dispersion analysis technique for a corrugated unit cell modelled in CST Microwave Studio™. The design guidelines available in literature suggest that a high-gain performance of this type of antenna, along with a satisfactory gain bandwidth can be achieved with $w > \lambda_0/2$ [23], [24].

The design process is demonstrated in Fig. 2 for a corrugated antenna of $r = 10$ rings as depicted in Fig. 1.b. The fixed depth of the first set of 5 rings is h_1, while the depth h_2 of the outer set of rings is a variable parameter. The dual-depth

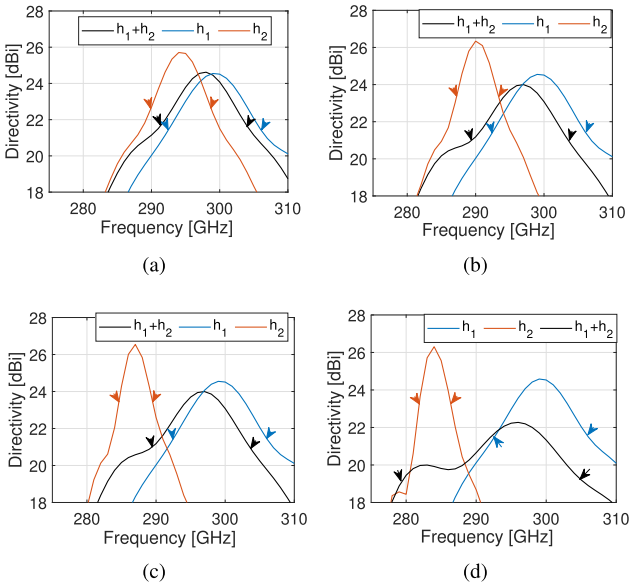

FIGURE 2. Simulated directivity of a dual-depth Bull's Eye antenna. It is $h_1 = 0.14$ mm and (a) $h_2 = 0.18$ mm, (b) $h_2 = 0.21$ mm, (c) $h_2 = 0.24$ mm and (d) $h_2 = 0.266$ mm. The colored arrows indicated the -3 dB directivity frequency points for each plot.

antenna is compared in directivity against the corresponding single depth antennas of the same size ($r = 10$) and is labelled as "$h_1 + h_2$" from now on. The depicted directivity and gain values are these of the main beam, radiating at broadside direction.

In the directivity plot of the dual-depth antenna, there can clearly be observed two peaks, each corresponding approximately to the central frequency determined by the rings with h_1 and h_2 from eq. (1). As h_2 obtains larger values, the 3-dB directivity bandwidth of the dual-depth antenna covers the frequency spectrum where radiation by the outer h_2 rings is stronger. The optimum model in terms of maximum directivity bandwidth, is shown in Fig. 2.d, where h_1 and h_2 are reasonably different and h_2 reaches the limit of $\lambda_0/4$ at around 300 GHz, as suggested by the known design parameters for corrugated metallic planes and relative theory [11]. Simulations showed that an effective transmission takes place only when $h_1 < h_2$ or, equivalently, it is compulsory that the first set of unit cells operates at the highest frequency. In particular, Fig. 3 depicts such a dual-depth antenna, when $h_1 = 0.24$ mm and $h_2 = 0.14$ mm. The achieved directivity of the dual-depth design is lower than the single depth antennas, with no elements of 3-dB directivity bandwidth expansion.

The proposed dual-depth model of Fig. 2.d, with $h_1 = 0.14$ mm and $h_2 = 0.266$ mm is further discussed below. For these selected values, dual-depth antennas of various sizes (from $r = 4$ to $r = 12$) are simulated and compared against single depth antennas of same design details (h_1, d, w) but different size r.

In Fig. 4, the dual-depth antenna of $r = 10$ is compared with the single $h_{1,2}$ antennas of the same maximum directivity and the same size. The 3-dB directivity bandwidth of the

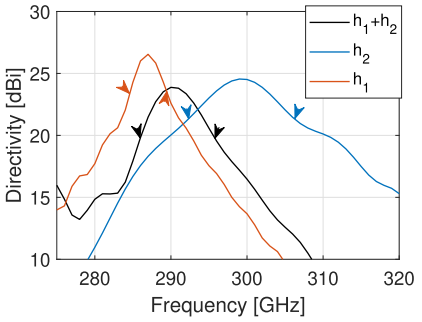

FIGURE 3. Simulated directivity of a dual-depth Bull's Eye antenna in comparison to single depth antennas when $h_1 > h_2$. It is $h_1 = 0.24$ mm, $h_2 = 0.14$ mm and the colored arrows indicated the -3 dB directivity frequency points for each plot.

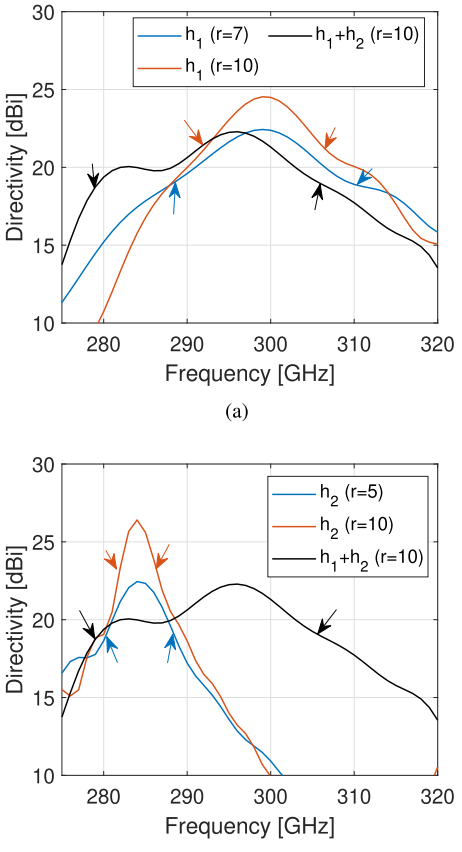

FIGURE 4. Comparison between three slot-fed Bull's Eye antennas of different sizes r. The dual depth antenna is compared with (a) the h_1 antenna and (b) the h_2 antenna. The colored arrows indicated the -3 dB directivity frequency points. It is $h_1 = 0.14$ mm and $h_2 = 0.266$ mm.

novel antenna lies exactly between the lower limit of the single h_2 directivity bandwidth and the upper limit of the single h_1 directivity bandwidth and is calculated at 8.6%. The fractional directivity bandwidth of the h_1 antenna with $r = 7$ (an antenna of similar maximum directivity) is 6.7%. It is denoted that the 3-dB fractional gain (directivity) bandwidth BW_{-3dB} is calculated according to the formula:

$$\%BW_{-3dB} = \frac{\Delta f_{-3dB}}{f_c} \tag{2}$$

TABLE 1. Comparison of slot-fed dual-depth antennas with standard corrugated antennas.

	r	3-dB Gain BW [%]	Max. Gain [dBi]
h_1	4	10.6	17.8
	5	8.4	19.8
	6	7	21
	7	6.7	22
	8	5.6	22.8
	9	5	23.5
	10	4.6	24
	11	4.4	24
	12	3.8	25
$h_1 + h_2$	4	**13.6**	18
	6	**9.34**	20
	8	**8.7**	21.2
	10	**8.6**	22
	12	**6.5**	22.8

where Δf_{-3dB} is the difference between the two frequency points that define the -3 dB gain (directivity) bandwidth and f_c is the central frequency of the -3 dB gain (directivity) spectrum.

In detail, the simulated farfield characteristics of each r-case antenna are summarized in Table 1. The antennas are compared in terms of size r, 3-dB fractional gain bandwidth and maximum gain. The comparison in these Tables is only between the dual-depth antenna and the single h_1 antenna, which is more broadband than the antenna of h_2 (as observed from Fig. 4). Only dual-depth designs of even number of rings are simulated, for the facilitation of the design process. A dual-depth design of an odd number of rings is feasible, and its performance is expected to lie between the adjacent presented designs of Table 1. Some notable trends of the dual-depth antenna are reported below:

- The dual-depth antenna of r rings achieves higher gain, compared to a single h_1 antenna of smaller size and similar 3-dB gain bandwidth. For example, for the dual-depth antenna of $r = 10$, there is an additional gain of 2.2 dBi compared to the single-depth antenna of $r = 5$, with both antennas exhibiting a similar 3-dB gain bandwidth around 8.5%.
- The dual-depth antenna provides 3% ($r = 4$), 2.6% ($r = 6$), 3.1% ($r = 8$) and 4% ($r = 10$) additional 3-dB gain bandwidth than a single h_1 antenna of the same size. This trend is observed however only for dual-depth designs of up to r=10. Simulations showed that dual-depth antenna sizes of $r > 10$ return to the typical performance of the single h_1 antennas of the same size r (see $r = 12$ at Table 1).
- The dual-depth antenna achieves 3% ($r = 4$), 1% ($r = 6$), 1.7% ($r = 8$) and 1.9% ($r = 10$) additional 3-dB gain bandwidth than a single h_1 antenna of similar maximum gain. The above remarks can be verified in Fig. 4, where the dual-depth antenna is compared with single-depth antennas of similar maximum directivity ($h_{1,r=7}$ in Fig. 4.a and $h_{2,r=5}$ in Fig. 4.b).

Table 2 summarizes the performance of our proposed dual-depth antennas compared to other known Bull's Eye antennas in literature. The antennas are compared in terms of number of rings r, 3-dB fractional gain bandwidth and peak gain. The well-known trade-off between gain/directivity bandwidth and maximum gain/directivity should be highlighted when comparing the results. Additionally, as noted in Section I, corrugated metallic designs can be directly scalable from microwave to THz frequencies, therefore all the presented designs of Table 2 are expected to perform similarly at different spectra, enabling a proper comparison. For example, our dual-depth antenna of $r = 6$ at 293 GHz, outperforms the existing antennas of $r = 7$ at millimeter-waves in both maximum gain and 3-dB gain bandwidth, with the additional advantage of smaller size (in free-space wavelengths). On the other hand, the design in [14] is of a very high gain, at the cost of a very large size and a narrow 3-dB gain bandwidth (only 3.6%). Our proposed designs offer a good compromise between antenna size, 3-dB gain bandwidth and maximum gain.

TABLE 2. Comparison between the proposed dual-depth antenna ($h_1 + h_2$) of different sizes r and antennas from literature.

	r	3-dB Gain BW [%]	Max. Gain [dBi]
[5], 16 GHz	6	11.5	18
[13], 96 GHz	7	7.5	17
[14], 77 GHz	20	3.6	29.38
[15], 60 GHz	7	3.3	19
[25], 60 GHz	7	8.26	19.7
$h_1 + h_2$, 296 GHz	10	8.6	22
$h_1 + h_2$, 296 GHz	8	8.7	21.2
$h_1 + h_2$, 293 GHz	6	9.34	20
$h_1 + h_2$, 293 GHz	4	13.6	18

The dual-depth corrugated antenna with $r = 10$ is selected as optimum case in terms of maximum gain (directivity), corresponding 3-dB bandwidth and size. A simulated radiation pattern comparison at the frequencies that determine the 3-dB gain bandwidth can be seen in Fig. 5. The comparison is between the dual-depth antenna of $r = 10$ and the h_1 and h_2 antennas of the same maximum directivity. At the lower limit of the 3-dB directivity spectrum, where the h_2 radiation dominates, the patterns of the dual-depth antenna are very similar with these of the single h_2 antenna. Likewise, at the frequencies of 0 dB, and upper 3-dB the $h_1 + h_2$ antenna exhibits similar patterns with the h_1 antenna. At angles around $\pm 20^o$ the E-planes of the dual-depth antenna show slightly higher side lobes, which is the effect of the set of rings with h_2. The contribution of the outer set of rings with h_2 at higher frequencies will be explained in the next section with an appropriate leaky wave analysis. We observed from simulations that the cross-polar patterns for both E- and H- planes exhibit a very low level below -60 dB. The worst case cross-polarization radiation pattern at 296 GHz occurs at a cut of $\phi = 45^o$ with values approximately -11 dB.

III. LEAKY WAVE ANALYSIS

It has been reported that corrugated metallic designs operate as leaky wave antennas, with a surface plasmon mode

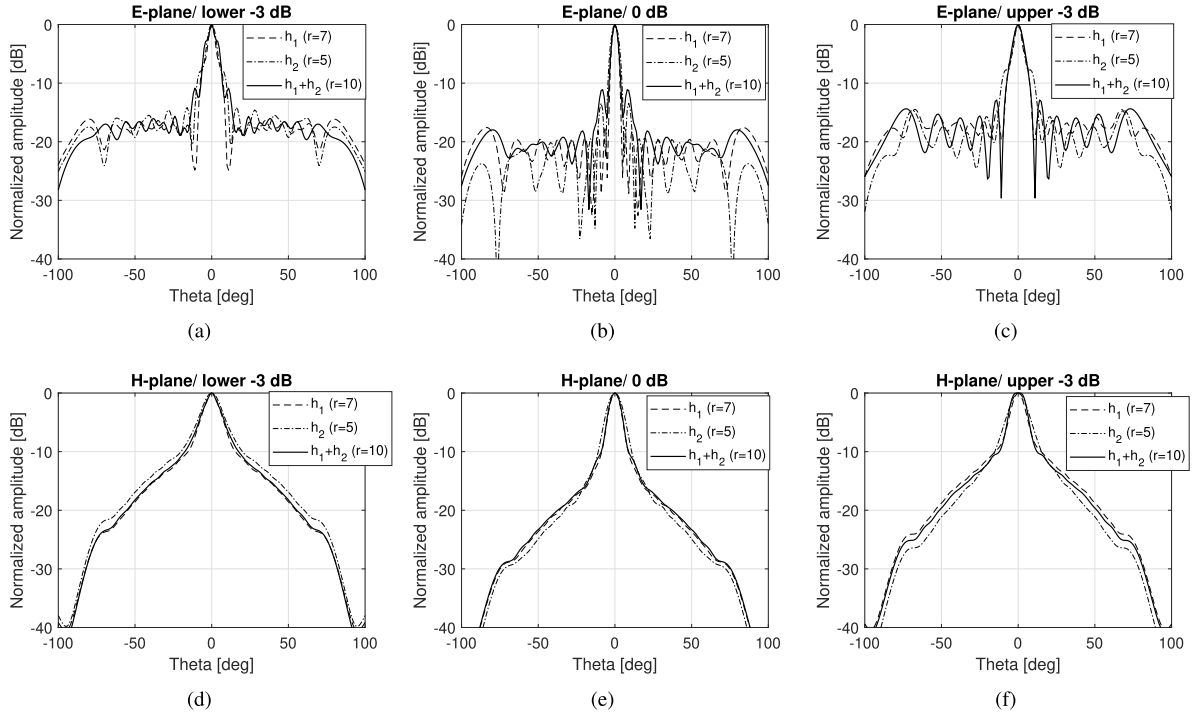

FIGURE 5. Simulated *E*- and *H*- planes at the 3-dB directivity spectrum of the dual-depth and the single-depth antennas of the same maximum directivity for $h_1 = 0.14$ mm and $h_2 = 0.266$ mm.

converting into a leaky wave as it propagates across the corrugations [4]. For the examined corrugated type of leaky wave antenna, the gaps of the corrugated antennas of Section II are large enough so that we can safely assume that a higher order mode (TM_1) is supported inside the gap, which is considered as a parallel-plate waveguide [26]–[28]. Although the fundamental *TEM* mode will still exist, it is expected to have attenuated significantly [28].

The wavenumber of the leaky mode of an infinitely long, one-dimensional, periodically corrugated metallic surface is extracted via the numerical solution of a transverse resonance equation at the level of the gap openings as [27], [28]:

$$Y_{in,TM} + Y_a(k_y) = 0 \tag{3}$$

where $Y_{in,TM}$ is the input admittance looking into the gap ($-z$ direction with reference to Fig. 1.b) for a *TM* shorted stub and Y_a is the admittance at the gap openings looking out of the gap ($+z$), calculated by the Parseval's theorem for transmission of power from the gap per unit length [27].

Below, a leaky wave analysis is performed for the h_1 corrugated plane and the h_2 corrugated plane, with all other design parameters as in Fig. 1. Due to the periodic formulation, the longitudinal guided wave (along $|y|$) consists of an infinite number of n space harmonics (Floquet modes) as:

$$k_{yn} = k_y + 2\pi n/d = \beta_n - j\alpha \tag{4}$$

where k_y is the wavenumber of the fundamental mode, d is the periodicity, β_n is the phase constant of the n-th harmonic and α is the attenuation constant. Since in these corrugated designs it is $d \approx \lambda_0$, the $n = -1$ harmonic is fast and induces the leaky wave phenomenon [20]. The phase constant of the leaky mode is associated with the angle θ of the main beam, according to:

$$\theta = \sin^{-1}(\beta_{-1}/k_0) \tag{5}$$

Fig. 6.a shows the propagation constant values for each single depth corrugated design. The TM_1 mode is dominant. The *TEM* mode exists only for the h_1 design at the depicted spectrum and has been calculated with the analytical periodic method of [28]. The *TEM* mode for the h_1 unit cells has been significantly attenuated at the examined spectrum, as shown in Fig. 6.b.

The following discussion refers only to the strongly excited TM_1 mode. Both designs are characterized by a fast wave ($|\beta_{-1}| < 1$) which scans from the backward to the forward quadrant. From the condition ($|\beta_{-1}| < \alpha$) for radiation at broadside for a finite size symmetrically-fed leaky-wave antenna, the h_2 antenna achieves maximum radiation around 287 GHz and the h_1 antenna around 303 GHz [29]. The steeper plot of β_{-1} for the h_2 design, indicates a quicker variation of the beam angle with frequency, therefore a quicker degradation of the main beam. This justifies the limited gain bandwidth of the h_2 antennas of Figs. 2,3 and 4. These results can be confirmed from the simulations of the finite-size models (see Fig. 2). A small shift in the frequency band of maximum radiated power for each antenna is expected due to the fact that the leaky wave analysis assumes infinite size antennas.

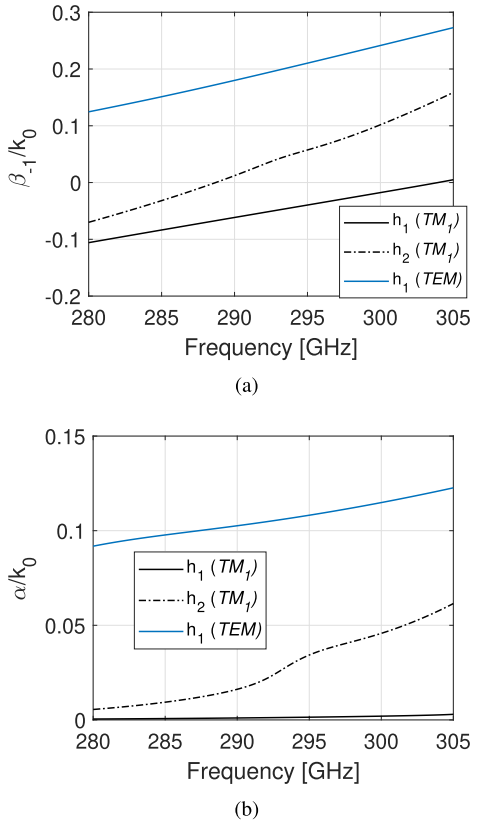

FIGURE 6. Leaky-wave analysis of each single-depth, one-dimensional, unidirectional corrugated plane with $h_1 = 0.14$ mm and $h_2 = 0.266$ mm. (a) Propagation constant. (b) Attenuation constant.

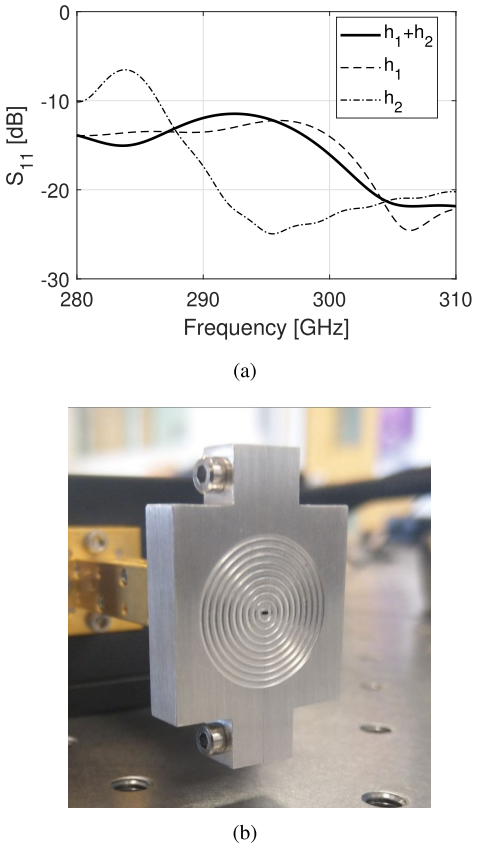

FIGURE 7. (a) Simulated S_{11} performance of Bull's Eye antennas with $r = 10$ with an open-ended waveguide aperture for $h_1 = 0.14$ mm and $h_2 = 0.266$ mm. (b) Fabricated prototype.

It is evident that the attenuation constant α increases with the increase of the depth h (Fig. 6.b). This implies that designs with large values of h, approach better the infinite size assumption, from the condition $L = 0.18\lambda_0/\alpha$, where L is the half-length of the antenna [20]. For larger depth values h, fewer unit cells are required for the infinite size assumption.

The aforementioned analysis can predict some characteristics of the farfield performance of the dual-depth antenna. At lower frequencies (around 285 GHz), the radiation of the h_2 antenna dominates (with $\beta_{-1} \approx 0$, therefore radiates at its maximum close to broadside), with the h_1 unit cells contributing with side lobes. At higher frequencies, the reverse farfield behaviour is observed. Also, for the dual-depth design, the maximum directivity is achieved at 295 GHz (Fig. 4.b), where the $|\beta_{-1}|$ values of each single depth design are the closest to 0 at the same time. These noted trends are verified by the simulated farfields of Fig. 5.

The high attenuation α of the h_2 design also explains why designs with large size ($r > 10$) do not benefit from the dual-depth concept, and exhibit a performance similar to the single depth h_1 antenna. The effect of the h_2 unit cells attenuates significantly with respect to h_1 unit cells, as r approaches the infinite size assumption.

IV. FABRICATION AND MEASUREMENTS

The proposed 10-ring dual-depth antenna of Section II, with $h_1 = 0.14$ mm and $h_2 = 0.266$ mm is selected as the optimum design to fabricate. In order to secure a steady, broadband matching performance at low THz and eliminate the fabrication challenges presented by a thin slot, the slot aperture of Section II is replaced with an open-ended waveguide aperture [19]. Its comparative advantages can be summarized as:

- A subwavelength aperture always requires a further optimization in its design process, while the design of an open waveguide is straightforward.
- At higher frequencies, fabrication of subwavelength dimensions can be quite challenging due to limitations of the fabrication tools. Therefore, a part with dimensions comparable to the wavelength facilitates the fabrication process.

Fig. 7.a confirms that an open-ended waveguide aperture antenna achieves S_{11} values below -10 dB at the frequency band between 275 GHz and 320 GHz. Table 3 compares three antennas with $r = 10$ rings and a waveguide aperture. The antennas are compared in terms of 3-dB gain bandwidth and maximum gain. From this Table, the same trends discussed previously can be observed for our proposed design. The maximum gain in all r cases is about 0.5 dBi lower than the corresponding slot-fed antennas of Table 1. The 3-dB gain bandwidth for the design of 10 rings is 8.85%.

TABLE 3. Dual-depth antenna with $r = 10$ and an open-ended waveguide aperture.

	r	3-dB Gain BW [%]	Max. Gain [dBi]
h_1	5	8.9	19.3
	7	5.3	21.8
	10	4.3	23.6
$h_1 + h_2$	10	**8.85**	21.3

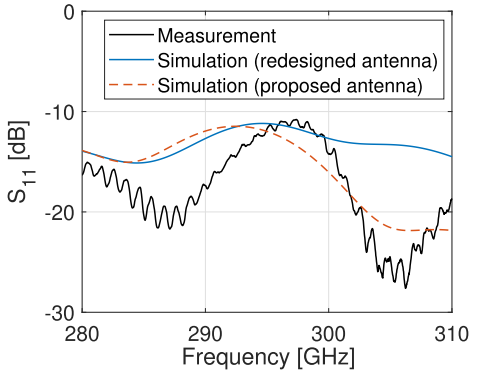

(a)

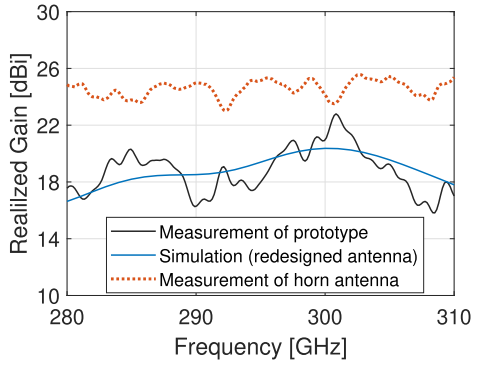

(b)

FIGURE 8. Measured versus simulated (a) S_{11} parameters and (b) realized gain of the waveguide aperture antenna.

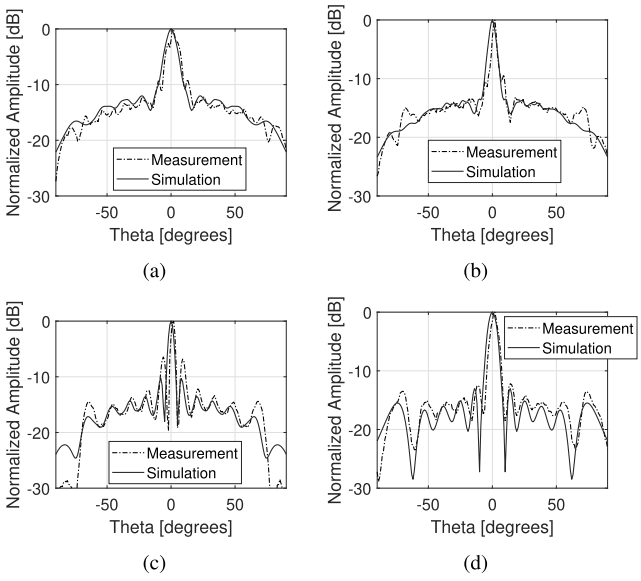

FIGURE 9. Measured *E*-plane radiation patterns at (a) 281.2 GHz, (b) 288.1 GHz, (c) 296 GHz, (d) 304.2 GHz.

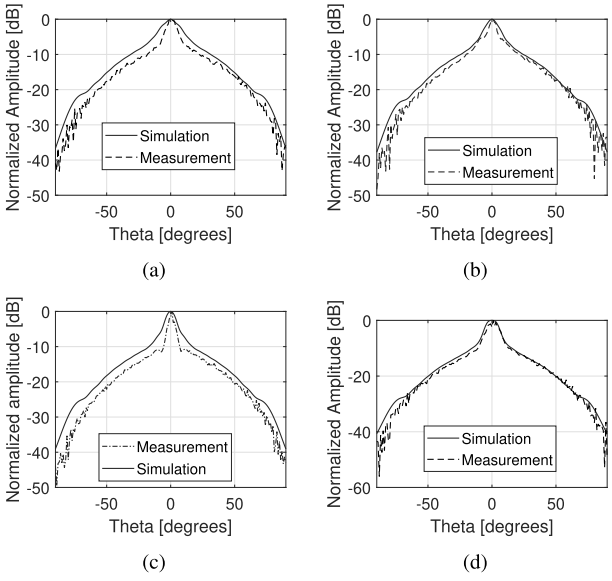

FIGURE 10. Measured *H*-plane radiation patterns at (a) 281.2 GHz, (b) 288.1 GHz, (c) 296 GHz, (d) 304.2 GHz.

The optimum dual-depth corrugated design was fabricated with an open-ended waveguide aperture. A three-axis CNC milling machine was used to create the indented rings on the surface of an aluminium plate with cutters of 0.2 mm diameter. The fabricated prototype can be seen in Fig. 7.b. The metallic plate was split in two halves across the E-plane of the waveguide, in order to ensure minimum disturbance of the main radiating mode. The two metallic blocks were joined back together with screws that were attached on two extra metal blocks added on both sides of the antenna. Additionally, the pins of the WR-3 flange had to fit entirely inside the ground plane, therefore the thickness of the ground plane had to be extended from its initial value of 0.91 mm to 7 mm. Simulations verified that such modifications did not affect the performance of the antenna.

The S_{11} parameters and the realized gain of the fabricated antenna were measured with a network analyser. For the realized gain measurement two reference horn antennas fed by a WR-3 waveguide were used, with an operational bandwidth from 282 GHz to 298 GHz.

Initial measurements demonstrated that the operation of the antenna was shifted towards higher frequencies, which implied some slight discrepancies for the dimensions of the fabricated prototype. A dimension measurement based on an infrared scan of the fabricated antenna revealed the actual details of the fabricated prototype. The fabricated antenna of Fig. 7.b has its dimensions as $d = 0.9728$ mm, $w = 0.562$ mm, $h_1 = 0.167$ mm and $h_2 = 0.302$ mm. The antenna was redesigned in CST Microwave Studio^{TM} and new simulated results were obtained (Figs. 8-9).

Fig. 8 shows the measured S_{11} parameters and realized gain compared to simulations of the redesigned antenna. A relatively good agreement between simulations and measurement can be observed. The measured S_{11} values are below -10 dB at all the measured frequencies. The plot of the measured gain shows two maxima of 22.5 dBi at 301 GHz and 20.5 dBi at 285 GHz, at the same frequencies as the redesigned simulated antenna. The observed ripples (less than 2 dB) in the realized gain are due similar variation of the gain of the reference horn antenna.

For the measurement of the radiation patterns of the antenna, a rotating base was used for a scanning from $-90°$ to $+90°$ with a resolution of $1°$. The Bull's Eye prototype was mounted on the rotating base, while a horn antenna was fixed at a farfield distance of about 1 m. The measured E-plane and H-plane radiation patterns compared to the simulated can be seen in Figures 9 and 10 for four different frequencies which cover all the 3-dB gain bandwidth of 25.4 GHz.

A good agreement is evident between measurements and simulations. In fact, the H-planes exhibit a slightly lower measured SLL than that expected from simulations. The E-plane radiation patterns, on the other hand, exhibit a slightly higher SLL compared to the simulations. These effects are attributed to slight misalignments and possible bending of the two metal split blocks that the antenna is made of.

V. CONCLUSION

A novel planar corrugated metallic antenna with significantly enhanced input matching and expanded 3-dB gain bandwidth has been proposed for enhanced transmission of power at low THz. The proposed dual-depth design utilises two different corrugation depths in an optimised configuration and is fed with a waveguide aperture at 300 GHz, achieving a 3-dB gain bandwidth of 8.85% and maximum directivity of 21.7 dBi (maximum gain 21.3 dBi), while keeping a low profile and a planar size of ten rings. The proposed antenna outperforms known implementations of similar size or gain. A leaky-wave analysis has been performed, allowing a physical insight into the operation of the dual-depth antenna. It is highlighted that a significant advantage of our proposed design methodology is its straightforward scaling to lower frequencies (mm-waves and microwaves), where fabrication of such antennas is facilitated by the availability of tools.

Simulated results were validated via a fabricated and measured prototype. A small frequency shift was observed between measurements and the initial design simulations, which is due to fabrication inaccuracies that have a significant effect in the low THz spectrum. Good agreement has been achieved between measurements and simulations of a redesigned model matching the exact dimensions of the fabricated prototype.

REFERENCES

[1] H. J. Lezec, A. Degiron, E. Devaux, R. A. Linke, L. Martin-Moreno, F. J. Garcia-Vidal, and T. W. Ebbesen, "Beaming light from a subwavelength aperture," *Science*, vol. 297, no. 5582, pp. 820–822, Aug. 2002.

[2] T. W. Ebbesen, H. J. Lezec, H. F. Ghaemi, T. Thio, and P. A. Wolff, "Extraordinary optical transmission through sub-wavelength hole arrays," *Nature*, vol. 391, no. 6668, pp. 667–669, Feb. 1998.

[3] L. Martín-Moreno, F. J. García-Vidal, H. J. Lezec, A. Degiron, and T. W. Ebbesen, "Theory of highly directional emission from a single subwavelength aperture surrounded by surface corrugations," *Phys. Rev. Lett.*, vol. 90, no. 16, Apr. 2003, Art. no. 167401.

[4] D. R. Jackson, A. A. Oliner, T. Zhao, and J. T. Williams, "Beaming of light at broadside through a subwavelength hole: Leaky wave model and open stopband effect," *Radio Sci.*, vol. 40, no. 6, Dec. 2005, Art. no. RS6S10.

[5] M. Beruete, I. Campillo, J. S. Dolado, J. E. Rodríguez-Seco, E. Perea, F. Falcone, and M. Sorolla, "Very low-profile 'Bull's eye' feeder antenna," *IEEE Antennas Wireless Propag. Lett.*, vol. 4, pp. 365–368, 2005.

[6] M. Beruete, U. Beaskoetxea, M. Zehar, A. Agrawal, S. Liu, K. Blary, A. Chahadih, X.-L. Han, M. Navarro-Cia, D. E. Salinas, A. Nahata, T. Akalin, and M. S. Ayza, "Terahertz corrugated and Bull's-eye antennas," *IEEE Trans. THz Sci. Technol.*, vol. 3, no. 6, pp. 740–747, Nov. 2013.

[7] J.-Q. Ding, J. Hu, S.-C. Shi, and Y. Zhao, "Beam shaping performance based on metallic corrugated grooves and dielectric periodic gratings at 500 GHz," *IEEE Access*, vol. 6, pp. 42507–42515, 2018.

[8] A. K. Nayak, V. Singh Yadav, and A. Patnaik, "Wideband transition from tapered microstrip to corrugated SIW," in *IEEE MTT-S Int. Microw. Symp. Dig.*, Dec. 2019, pp. 1–4.

[9] Y. Lin, Y. Zhang, H. Liu, Y. Zhang, E. Forsberg, and S. He, "A simple high-gain millimeter-wave leaky-wave slot antenna based on a bent corrugated SIW," *IEEE Access*, vol. 8, pp. 91999–92006, 2020.

[10] M. N. M. Kehn and C. Z. Chen, "Analysis of leaky-wave radiation from corrugated parallel-plate waveguides with steerable beams by rotatable corrugations," *IEEE Trans. Antennas Propag.*, early access, Apr. 5, 2021, doi: 10.1109/TAP.2021.3069545.

[11] M. Beruete, M. Sorolla, I. Campillo, J. S. Dolado, L. Martín-Moreno, J. Bravo-Abad, and F. J. García-Vidal, "Enhanced millimeter-wave transmission through subwavelength hole arrays," *Opt. Lett.*, vol. 29, no. 21, p. 2500, 2004.

[12] M. B. Diaz, I. Campillo, J. S. Dolado, J. E. Rodríguez-Seco, E. Perea, F. Falcone, and M. S. Ayza, "Dual-band low-profile corrugated feeder antenna," *IEEE Trans. Antennas Propag.*, vol. 54, no. 2, pp. 340–350, Feb. 2006.

[13] U. Beaskoetxea, S. Maci, M. Navarro-Cía, and M. Beruete, "3-D-printed 96 GHz Bull's-eye antenna with off-axis beaming," *IEEE Trans. Antennas Propag.*, vol. 65, no. 1, pp. 17–25, Jan. 2017.

[14] U. Beaskoetxea, V. Pacheco-Peña, B. Orazbayev, T. Akalin, S. Maci, M. Navarro-Cía, and M. Beruete, "77-GHz high-gain Bull's-eye antenna with sinusoidal profile," *IEEE Antennas Wireless Propag. Lett.*, vol. 14, pp. 205–208, 2015.

[15] U. Beaskoetxea and M. Beruete, "High aperture efficiency wide corrugations Bull's-eye antenna working at 60 GHz," *IEEE Trans. Antennas Propag.*, vol. 65, no. 6, pp. 3226–3230, Jun. 2017.

[16] S. Alkaraki, Y. Gao, and C. Parini, "Dual-layer corrugated plate antenna," *IEEE Antennas Wireless Propag. Lett.*, vol. 16, pp. 2086–2089, 2017.

[17] C. H. Gan and G. Gbur, "Extraordinary optical transmission through multilayered systems of corrugated metallic thin films," *Opt. Exp.*, vol. 17, no. 22, pp. 20553–20566, 2009.

[18] H. B. Chan, Z. Marcet, K. Woo, D. B. Tanner, D. W. Carr, J. E. Bower, R. A. Cirelli, E. Ferry, F. Klemens, J. Miner, C. S. Pai, and J. A. Taylor, "Optical transmission through double-layer metallic subwavelength slit arrays," *Opt. Lett.*, vol. 31, no. 4, p. 516, 2006.

[19] D. Kampouridou and A. Feresidis, "Effects of the feeding structure on low-THz Bull's eye antennas," in *Proc. IET Conf. Publications*, 2018, pp. 1–5.

[20] D. R. Jackson and A. A. Oliner, "Leaky-wave antennas," in *Modern Antenna Handbook*, C. Balanis, Ed. New York, NY, USA: Wiley, 2008.

[21] F. J. García-Vidal and L. Martín-Moreno, "Transmission and focusing of light in one-dimensional periodically nanostructured metals," *Phys. Rev. B, Condens. Matter*, vol. 66, no. 15, Oct. 2002, Art. no. 155412.

[22] M. Beruete, I. Campillo, J. S. Dolado, J. E. Rodríguez-Seco, E. Perea, and M. Sorolla, "Enhanced microwave transmission and beaming using a subwavelength slot in corrugated plate," *IEEE Antennas Wireless Propag. Lett.*, vol. 3, pp. 328–331, 2004.

[23] M. Beruete, U. Beaskoetxea, and T. Akalin, "Flat corrugated and bull's-eye antennas," in *Aperture Antennas for Millimeter and Sub-Millimeter Wave Applications* (Signals and Communication Technology), A. Boriskin and R. Sauleau, Eds. Cham, Switzerland: Springer, 2018.

[24] D. Kampouridou and A. Feresidis, "Full-wave leaky-wave analysis of 1-D periodic corrugated metal surface antennas," *IEEE Antennas Wireless Propag. Lett.*, vol. 20, no. 5, pp. 863–867, May 2021.

[25] C. J. Vourch and T. D. Drysdale, "V-band 'Bull's eye' antenna for CubeSat applications," *IEEE Antennas Wireless Propag. Lett.*, vol. 13, pp. 1092–1095, 2014.
[26] D. Y. Na, K. Y. Jung, and Y. B. Park, "Transmission through an annular aperture surrounded with corrugations in a PEC plane," *IEEE Antennas Wireless Propag. Lett.*, vol. 14, pp. 179–182, 2015.
[27] D. Kampouridou and A. Feresidis, "Dispersion analysis of 1-D periodic corrugated metallic surfaces," in *Proc. IET Conf. Publications*, 2018, pp. 1–2.
[28] A. Sutinjo and M. Okoniewski, "A simple leaky-wave analysis of 1-D grooved metal structure for enhanced microwave radiation," *IEEE Trans. Antennas Propag.*, vol. 60, no. 6, pp. 2719–2726, Jun. 2012.
[29] P. Burghignoli, G. Lovat, and D. R. Jackson, "Analysis and optimization of leaky-wave radiation at broadside from a class of 1-D periodic structures," *IEEE Trans. Antennas Propag.*, vol. 54, no. 9, pp. 2593–2604, Sep. 2006.

DESPOINA KAMPOURIDOU (Member, IEEE) was born in Greece, in 1990. She received the degree in electrical and computer engineering from the Aristotle University of Thessaloniki, Greece, in 2015, and the Ph.D. degree in electronic, electrical, and systems engineering from the University of Birmingham, U.K., in 2020.

During 2018, she was a Research Associate, and since 2019, she has been a Research Fellow with the Department of Electrical, Electronic and Systems Engineering, University of Birmingham. In 2020, she was awarded the Royal Academy of Engineering U.K. Intelligence Community Postdoctoral Research Fellowship, from 2020 to 2022. Her research interests include analysis and design of metamaterials, leaky-wave antennas, dispersion analysis methods, and microwave circuits. She is a member of the Technical Chamber of Greece.

ALEXANDROS FERESIDIS (Senior Member, IEEE) was born in Thessaloniki, Greece, in 1975. He received the degree in physics from the Aristotle University of Thessaloniki, Greece, in 1997, the M.Sc. (Eng.) degree in radio communications and high frequency engineering from the University of Leeds, U.K., in 1998, and the Ph.D. degree in electronic and electrical engineering from Loughborough University, U.K., in 2002.

During the first half of 2002, he was a Research Associate and in the same year he was appointed to a Lecturer in wireless communications with the Department of Electronic and Electrical Engineering, Loughborough University, U.K., where, in 2006, he was promoted to a Senior Lecturer. In December 2011, he joined the Department of Electronic, Electrical and Systems Engineering, University of Birmingham, U.K., where he is currently a Reader. He has published more than 150 articles in peer reviewed international journals and conference proceedings and has coauthored three book chapters. His research interests include analysis and design of metamaterials, electromagnetic band gap (EBG) structures and frequency selective surfaces (FSS), leaky-wave antennas, small/compact antennas, passive microwave/mm-wave/THz circuits, microfabrication, numerical techniques for electromagnetics, and bioelectromagnetics.

Dr. Feresidis is a member of the U.K. EPSRC Peer Review College, he was on the Editorial Board of *IET Microwaves* and *Antennas and Propagation journal*, from 2014 to 2018. He has held a Senior Research Fellowship Award from the U.K. Royal Academy of Engineering and The Leverhulme Trust, from 2013 to 2014. He is currently an Associate Editor of the IEEE TRANSACTIONS ON ANTENNAS AND PROPAGATION.